STUDY OF MULTIPOLAR RF KICKS FROM THE MAIN DEFLECTING MODE IN COMPACT CRAB CAVITIES FOR LHC*

J. Barranco García, R. Calaga, R. De Maria, M. Giovannozzi, A. Grudiev, R. Tomás
CERN, Geneva, Switzerland

Abstract

A crab cavity (CC) system is under design in the framework of the High Luminosity LHC project. Due to transverse space constraints on one hand and the RF frequency requirements on the other hand, the design of the crab cavities has to be compact. This results in the crab cavity shape being far from axially symmetric and, as a consequence, higher order multipolar components of the main deflecting mode are non-zero. In this paper, multipolar RF-kicks from the main deflecting mode are calculated in the compact CC for LHC. They are compared to the multipolar error in LHC magnets. The possible influence of the RF-kicks on the beam dynamics has been investigated by means of analytical estimates.

MULTIPOLAR RF KICK CALCULATION

Geometry of the LHC CC Prototypes

In Fig 1, geometry of the three prototypes of the LHC CC are shown: (left) Ridged Waveguide cavity (RWCAV) [1]; (middle) Quarter Wave resonator cavity (QWCAV) [2]; (right) 4 rod resonator cavity (4RCAV) [3]. They exploit different ways to make a 400 MHz deflecting cavity so compact that it fits in the space available between two beam pipes of the LHC interaction regions [4]. Nevertheless, in all three cases, geometry of the cavity is axially non-symmetric giving rise to higher order multipolar components of the main deflecting mode.

Electro-Magnetic Field Representation of the Main Deflecting Mode

In an axially symmetric deflecting cavity, the main dipole mode (m=1) has only dipolar variation of the electro-magnetic field ~exp(inφ), where n=m=1. It is not the case, however, for the LHC CC prototypes shown in Fig. 1 due to strong deviation of the cavity shape from the axially symmetric one. In this case, all multipolar components n ≥ 1 are present depending on the cavity symmetry. In order to simplify the math we assume that all cavities are symmetric with respect to the horizontal plane XZ and are oriented in such a way that dipolar kick is in X direction. This is true all three cavities shown in Fig 1. In this case, all skew components are zero and azimuthal dependence is ~cos(nφ). Furthermore, assuming that the particle of charge e moves parallel to the Z-axis with the speed of light c, the perpendicular Lorentz force acting on it can be expressed as follows:

$$F_\perp = e\left[E_{kick} + Z_0 \vec{u}_z \times H_{kick}\right]$$

where Z_0 is vacuum impedance, u_z the unit vector in Z direction, $E_{kick} = E_\perp \cdot e^{j\omega z/c}$; $H_{kick} = H_\perp \cdot e^{j\omega z/c}$ are the electric and magnetic fields in the particle frame, respectively, while $E_\perp$ and $H_\perp$ are the corresponding electric and magnetic fields in the cavity frame. These fields can be expressed as a sum of multipoles similarly to what is done for magnets [5]. Then, the perpendicular Lorentz force is expressed as a sum over its multipolar components $F_\perp^{(n)}$:

$$F_\perp(r,\varphi,z) = \sum_{n=1}^{\infty} F_\perp^{(n)}(z) r^{n-1}[\vec{u}_r \cos(n\varphi) + \vec{u}_\varphi \sin(n\varphi)]$$

Furthermore the transverse momentum change of the particle when traversing the cavity, i.e., the kick is given by

$$\Delta p_\perp(r,\varphi) = \frac{1}{c}\int_0^L F_\perp dz = \sum_{n=1}^{\infty} \Delta p_\perp^{(n)}(r,\varphi)$$

where

$$\Delta p_\perp^{(n)} = \frac{1}{c} r^{n-1}[\vec{u}_r \cos(n\varphi) + \vec{u}_\varphi \sin(n\varphi)]\int_0^L F_\perp^{(n)} dz \qquad (1)$$

are the multipolar components of the RF-kick expressed in terms of the transverse EM fields integrated over the cavity length L. They can also be expressed in terms of multipolar components of the accelerating field, namely, $E_{acc} = E_z \cdot e^{j\omega z/c} = \sum_n E_{acc}^{(n)} r^n \cos(n\varphi)$ using Panofsky-Wenzel (PW) theorem:

$$\Delta p_\perp(r,\varphi) = \frac{je}{\omega}\int_0^L dz[\nabla_\perp E_{acc}(r,\varphi,z)]$$

In this case:

$$\Delta p_\perp^{(n)} = \frac{je}{\omega} n r^{n-1}\left[\vec{u}_r \cos(n\varphi) + \vec{u}_\varphi \sin(n\varphi)\right]\int_0^L E_{acc}^{(n)}(z) dz \qquad (2)$$

Comparison of $\Delta p_\perp^{(n)}$ calculated from Eqs. (1) and (2) gives an estimate of numerical accuracy. Finally for ultra-relativistic particle the transverse RF-kick strength can be equated to a magnetic kick of the same strength:

$$b_n = \int_0^L B^{(n)} dz \text{ where } B^{(n)} = \frac{1}{ec} F_\perp^{(n)} = \frac{nj}{\omega} E_{acc}^{(n)} .$$

This expression is useful for comparing the strength of RF and magnetic multipoles in the same units. Although RF and magnetic multipoles can be compared, there is an essential difference. Magnetic multipoles are static and the corresponding kick does not depend on the longitudinal position of particles, whereas RF multipoles are harmonically oscillating at f_{RF}, i.e., at 400 MHz in the LHC case, and the corresponding kick depends on the RF

*The research leading to these results has received funding from the European Commission under the FP7 project HiLumi LHC, GA no. 284404, co-funded by the DoE, USA and KEK, Japan.

ISBN 978-3-95450-115-1

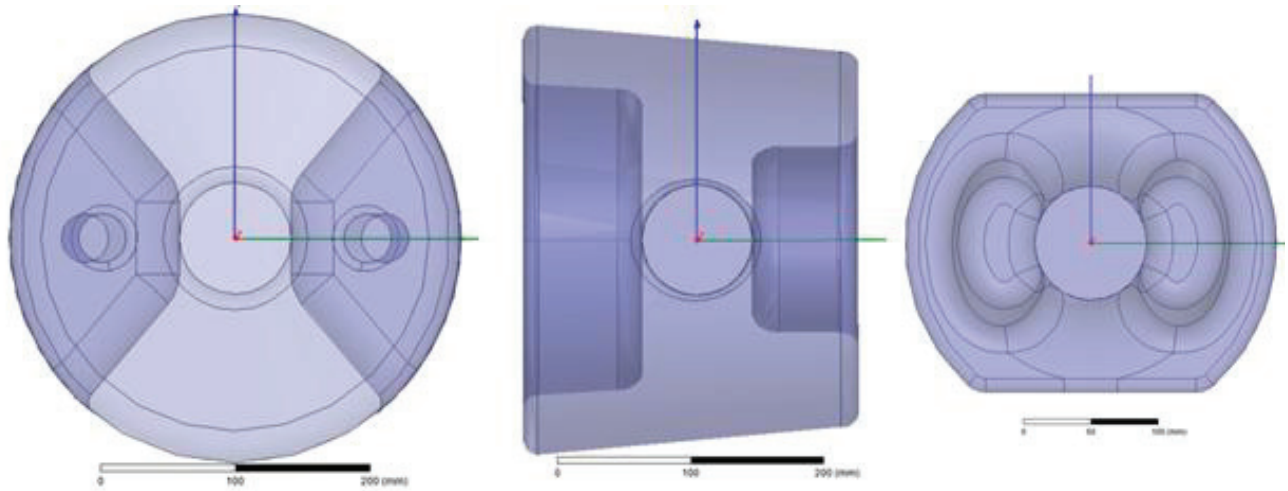

Figure 1: Geometry of the LHC CC prototypes: RWCAV (left), QWCAV (middle), 4RCAV (right).

phase of particles. Consequently, RF multipoles b_n are complex numbers, with the real part being the kick to a particle at the deflecting RF phase and the imaginary part being the kick to a particle at crabbing RF phase. The RF-kick to a particle at arbitrary RF phase difference from the crabbing RF phase $\delta\phi_{CC}$ is given as:

$$\Delta p_{\perp}^{(n)} = \Im\left\{er^{n-1}\left[\vec{u}_r \cos(n\varphi) + \vec{u}_\varphi \sin(n\varphi)\right] b_n e^{j\delta\phi_{CC}}\right\}.$$

Multipolar RF Kicks in LHC CC Prototypes

EM field maps have been calculated for the three cavity geometries presented in Fig. 1 using frequency domain finite element code HFSS [6]. Then the integrated strength of the RF multipoles has been calculated in two different ways using Eqs. (1) and (2). Comparing these two values, the relative accuracy of the calculations is estimated to decrease from few per mille for n=3 down to few per cent for n=7. Finally, values of the multipoles calculated at the nominal deflecting voltage V_{CC} = 10 MV using Eq (1) are summarized in Table 1. There are a few things worth mentioning: due to symmetry all even multipoles are zero in RWCAV and 4RCAV; in QWCAV, which has no symmetry with respect to the plane YZ, all multipoles are present. Last but not least, the imaginary part of all calculated multipoles in all three cavities is zero within the accuracy of the calculation. In other words, higher order multipoles (n>1) are in phase with the main dipole component (n=1) and there is no transverse kick acting on a particle at the crabbing phase.

In order to give a scale to the RF multipolar strength for LHC CC prototypes, they are compared to the rms field quality of the D2 separation dipoles that are currently installed in the LHC ring in IR1 and IR2 [7]. It is interesting to note that both the magnetic and the RF multipoles are of the same order of magnitude. This means that a careful analysis of the impact of the CC field quality is mandatory, both in terms of analytical indicators of the beam dynamics (see next section) and in terms of numerical simulations of the long-term impact on the beam dynamics.

Table 1: Values of the multipolar RF kick coefficients for LHC CC prototypes at nominal deflecting voltage: V_{CC} = 10MV and of the D2 separation dipole (MBRC) for reference (b_n is in units of mTm/m^{n-1}).

	MBRC	RWCAV	QWCAV	4RCAV
b_2	55	0	114	0
b_3	7510	3200	1260	900
b_4	82700	0	1760	0
b_5	2.9×10^6	-0.52×10^6	-0.15×10^6	-2.44×10^6
b_6	52×10^6	0	-1.66×10^6	0
b_7	560×10^6	-140×10^6	0	-650×10^6

BEAM DYNAMICS

The presence of RF multipolar kicks will introduce different type of beam dynamics perturbations according to their order. The aberrations considered include up to the octupolar component:

- Linear tune shift
$$\Delta Q_{x,y} = \frac{1}{4\pi}\beta_{x,y}\frac{b_2}{B\rho},$$
- chromaticity shift
$$\Delta\xi_{x,y} = \frac{\pm1}{4\pi}D_x\beta_{x,y}\frac{2b_3}{B\rho},$$
- coupling
$$\Delta Q_{min} = \frac{1}{2\pi}\sqrt{\beta_x\beta_y}D_y\frac{2b_3}{B\rho}\delta,$$
- Amplitude detuning, generating a tune shift at 3σ (the coupling term is not considered here)
$$\Delta Q_{x,y} = \frac{3}{8\pi}\beta_{x,y}^2\frac{b_4}{B\rho}9J_{x,y}$$

where $\beta_{x,y}$, D_y are the beta and vertical dispersion functions at the location of the CC and $J_{x,y}$, δ, $B\rho$ are the action, relative momentum error and beam rigidity of the particle, respectively. For simplicity, in the analytical estimate of the different aberrations the multipoles are considered to be static, i.e., the longitudinal dependence is omitted and only the modulus of the phasor is used. The SLHC3.1b lattice version is used [8], considering a local crab cavity scheme with vertical crossing at IP1 and horizontal crossing at IP5. A crab cavity voltage of V_{CC} = 10 MV is needed to provide a longitudinal tilt to the bunch of 260 μrad at the IP. The optical parameters at the location of each cavity for Beam 1 are shown in Table 2.

Table 2: Optics functions at the location of the three crab cavities to be installed in each side of the high-luminosity insertions IR1/5 for Beam 1 (CC3 is the cavity nearest to the IP).

Side		CC1	CC2	CC3
Left	$\beta_{x,y}$ [km]	3.47/2.92	3.56/3.16	3.65/3.42
	$D_{x,y}$ [m]	0.1/0.0	0.1/0.0	0.1/0.0
Right	$\beta_{x,y}$ [km]	2.79/3.43	3.04/3.52	3.29/3.61
	$D_{x,y}$ [m]	-0.1/0.0	-0.1/0.0	-0.1/0.0

The aberrations computed for the multipolar coefficients listed in Table 1 using the optical conditions of Table 2, where the maximum optical parameters between the left and right side of the insertions are used, are listed in Table 3. It is worth recalling that the CC installed in IR1 (vertical crossing) will feature also an a_3, generated by the rotation of the original b_3 component by 90 degrees, whose effect is not estimated here. The linear tune shift for the QWCAV type is found to be large. This is going to generate a tune modulation, whose amplitude is larger than in existing machines like SPS, HERA. The operational experience suggested that any tune modulation should be kept smaller than $\Delta Q_{max} \sim 10^{-4}$ [9]. Parenthetically, this criterion has been used to specify the performance of the LHC power converters.

Table 3: Evaluation of the possible beam aberrations induced by the CC installed in one side of one IR in which we assume a horizontal crossing plane.

	RWCAV	QWCAV	4RCAV
$\lvert\Delta Q_{x,y}\rvert[10^{-3}]$	0	1.4	0
$\lvert\Delta \xi_{x,y}\rvert[10^{-3}]$	7.96	3.13	2.24
$\lvert\Delta Q\rvert[10^{-6}]$	0	5.06	0

The coupling is zero by design for this particular optical configuration as the vertical dispersion at the location of the CC is zero. The values of the higher-order aberrations for the crab cavities are comparable with those of the D2 separation dipole.

CONCLUSIONS

A formalism characterizing the non-linearity of deflecting RF field has been applied to the LHC compact crab cavity prototypes in a similar way as it is done for magnets. The multipolar components of the EM field have been calculated for the LHC CC prototypes and found comparable to the field quality of the D2 separation dipole of the nominal LHC machine. First estimates of the effect of CC field quality on beam dynamics have been carried out. Assuming static perturbations, the linear tune shift, the chromaticity shift and the amplitude detuning have been estimated for the three CC layouts. The tune modulation from the QWCAV could be a source of concern. It is worth stressing that such analytical estimates are only indicators of what could be the situation. In reality, the long-term effect on the beam dynamics should be checked with detailed numerical simulations. Recent developments in the MAD-X [10] and the SixTrack codes have made it possible to perform such simulations in the near future.

ACKNOWLEDGMENT

We would like to thank L. Deniau, A. Latina, and F. Schmidt for their support in implementing the changes in MAD-X and SixTrack required for long-term CC simulations. Useful discussions and suggestions by S. Fartoukh are warmly acknowledged.

REFERENCES

[1] J. R. Delayen et. al., "Ridged Waveguide & Modified Parallel Bar," Presented at 5th LHC CC workshop, Geneva, 2011.
[2] I. Ben-Zvi et. al., "Quarter Wave Resonator," Presented at 5th LHC CC workshop, Geneva, 2011.
[3] G. Burt et. al., "4 Rod RF Design," Presented at 5th LHC CC workshop, Geneva, 2011.
[4] R. De Maria and S. Fartoukh, "Optics and layout for the HL-LHC upgrade project with a local crab cavity scheme," sLHC-Project-Report-55, 2011.
[5] D. A. Goldberg and G. R. Lambertson, "Dynamic devices: A Primer on Pickups and Kickers," AIP Conf. Proc. 249 (1992) 537.
[6] Ansys HFSS; http://www.Ansys.com
[7] P. Hagen, "WISE – User Guide and Implementation Notes," LHC-Project-Report-1056, 2008.
[8] S. Fartoukh and R. De Maria, "Optics and Layout Solutions for HL-LHC with Large Aperture Nb3Sn and Nb-Ti Inner Triplets," MOPPC011, these proceedings.
[9] F. Bordry, R. Schmidt, A. Verdier, "Power Converter Noise and Tune Modulation at the LHC Due to the Low-B Quadrupoles," LHC-Project-Note-98.
[10] L. Deniau and A. Latina, "Evolution of MAD-X in the framework of LHC upgrade studies," MOPPC076, these proceedings.

ISBN 978-3-95450-115-1